ELSEVIER

Biosensors & Bioelectronics 16 (2001) 491–501

BIOSENSORS & BIOELECTRONICS

www.elsevier.com/locate/bios

A biosensor for detecting changes in cognitive processing based on nonlinear systems analysis

Ghassan Gholmieh [a], Walid Soussou [b], Spiros Courellis [a], Vasilis Marmarelis [a], Theodore Berger [a,b], Michel Baudry [a,b,*]

[a] *Department of Biomedical Engineering, University of Southern California, Los Angeles, CA 90089-1451, USA*
[b] *Neuroscience Program, HNB124, University of Southern California, Los Angeles, CA 90089-2520, USA*

Abstract

A new type of biosensor, based on hippocampal slices cultured on multielectrode arrays, and using nonlinear systems analysis for the detection and classification of agents interfering with cognitive function is described. A new method for calculating first and second order kernel was applied for impulse input–spike output datasets and results are presented to show the reliability of the estimations of this parameter. We further decomposed second order kernels as a sum of nine exponentially decaying Laguerre base functions. The data indicate that the method also reliably estimates these nine parameters. Thus, the state of the system can now be described with a set of ten parameters (first order kernel plus nine coefficients of Laguerre base functions) that can be used for detection and classification purposes.

Keywords: Biosensor; Hippocampal slice; Nonlinear systems analysis

1. Introduction

From antiquity to modern times, there has been a need for detecting threats in the environment. This need is even more acute nowadays as increased environmental pollution as well as activities of groups of terrorists or of various types of fanatics (as illustrated by the attack of the Tokyo subway; Falkenrath et al., 1998; Tucker, 2000) cause serious threats to the general population. Analytical systems have become extremely sensitive and discriminative and are effective sensors as long as the nature of the detected agent is known. This is, in particular, the case of the MM1 (Rostker, 1997), the M22 ACADA, for automatic Chemical Agent Detector (http://www.gulflink.osd.mil/campmont/index.html) or a hybrid technology system, the M90-D1-C (Environics, Milliken, Finland). Even then, such systems do not provide much information on the biological effects of the detected agent. Biological systems, in principle at least, provide ideal detectors and reporters for environmental threats, as they are complex systems, which have evolved to maintain homeostasis despite continuously changing environments. Moreover, they do provide information regarding the biological effects of the perturbing agents. The problem is made more difficult when the agents to be detected affect cognitive processes. In this case, the detection requires either sophisticated behavioral tests not easily implemented in a biosensor, or indirect assays that are strongly indicative of potential cognitive dysfunction. We have developed a biosensor consisting of a multi-electrode array monitoring the functioning of complex neuronal networks contained in a cortical structure involved in cognitive processing. The underlying assumption is that agents that affect hippocampal function will also affect cognitive function in humans.

The evolution of multi-electrode array (MEA) recording from an experimental project to a routine physiological tool makes it possible to study spatially extended populations of interconnected neurons (i.e. networks) in brain slices (Gross, 1979; Pine, 1980; Gross et al., 1982, 1985, 1993; Novak and Wheeler, 1988; Boppart et al., 1992; Meister et al., 1994; Stoppini et al., 1997; Egert et al., 1998; Maher et al., 1999; Oka

* Corresponding author. Tel.: +1-213-740-9188; fax: +1-213-740-5687.
E-mail address: baudry@neuro.usc.edu (M. Baudry).

0956-5663/01/$ - see front matter
PII: S0956-5663(01)00163-4

et al., 1999). With a large number of appropriately spaced electrodes, and appropriate support hardware, it is possible to design input patterns with the spatio-temporal richness needed to activate complex network activity. The present data indicate that random train stimulation consisting of as few as 400 impulses delivered over 200 s is sufficient to accurately determine high order kernels, which are a mathematical expression of the nonlinearities of the network. Both theoretical and experimental work indicates that any agent affecting neuronal function will produce a distinct modification of higher order kernels (Scalabassi et al., 1988). Having 64 electrodes in the arrays ensures that there is always a sufficient number of pairs of stimulating/recording electrodes to perform random train stimulation and kernel analysis within each slice (our current experience indicates that as many as four kernels can be obtained from one stimulation site). Furthermore, pairs of stimulating/recording electrodes can be located in different hippocampal subfields, thus providing for an additional spatial parameter that can be used to further characterize the effect of an agent on the state of the system. Thus, not only does random train stimulation offers a rapid way of detecting the presence of a potentially hazardous agent, but it also provides unique information about this agent. By comparison with a known library of molecules, it will be possible to identify the agent itself, or, if not, its site of action. We also present an outline of how our analysis will provide for an efficient classification system for any molecule tested with our system.

2. Materials and methods

2.1. Hippocampal slice preparation

2.1.1. Acute slices

Adult rats were anesthetized with halothane and decapitated. The brain was quickly removed and bathed in an ice-cold aCSF (NaCl, 128 mM; KCl, 2.5 mM; NaH_2PO_4, 1.25 mM; $NaHCO_3$, 26 mM; Glucose, 10 mM; $MgSO_4$, 2 mM; ascorbic acid, 2 mM; $CaCl_2$, 2 mM aerated with 95% O_2/5% CO_2). The hippocampus was dissected out and transverse slices (thickness 400–500 μm) were collected using a Leika vibratome (VT 1000S). They were left to equilibrate for at least 1 h in aCSF (containing 2 mM Mg) at room temperature. During the recording session, a slice was transferred to the multielectrode plate (multielectrode array setup (MEA) or multimicroelectrode plate setup (MMEP) and was held down using a metallic ring and a string mesh. The slices were perfused with an aCSF containing a lower concentration of magnesium (1 mM). The slice was positioned carefully over the array with the help of an inverted microscope (4 × magnification, Leica DML, Leika DM IRB). After documenting the relative position of the slice with respect to the array with an analogue camera (Analogue Hitachi VK-C370, Digital Spot Model 2.0.0), the slice was left for 15 min to equilibrate again. Biphasic current stimulation was achieved using either intrinsic microelectrodes (MEA setup) or an external bipolar Nichrome electrode (MMEP set up).

2.1.2. Cultured slices

A modified version of the roller technique originally described by Gahwiler (1981) was used to culture hippocampal slices on both the MEA and MMEP set-ups. Briefly, hippocampal slices (400 μm thick) were prepared from 7-day-old rats with a McIllwain tissue slicer. Slices were glued over multielectrode arrays using a combination of thrombin (10 μl, 50 units/ml, Sigma) and plasma (10 μl, Sigma). The slices were left for 5 min in order to form a rigid clot. A volume of 3 ml of culture medium was added to the MEA arrays and slices were covered with their respective caps (ALA scientific). The MMEP array, on the other hand, was positioned in a large covered 7 cm diameter Petri dish. Fourteen milliliters of culture medium was added. One liter of culture medium contained Basal Medium Eagle (Sigma B-9638, 4.6 g), Earle Balanced Salts (Sigma E-6132, 2.17 g), and 33% Horse Serum (Gemini-Bio-Products # 100-105). The medium was supplemented by adding: NaCl, 15 mM; ascorbic acid, 0.4 mM; glucose, 36 mM; HEPES, 20 mM; $CaCl_2$, 150 μM; $MgSO_4$, 1.2 mM; glutamine, 2 mM; insulin (1 mg/100 ml); and 3 ml penicillin/streptomycin (Gibco BRL # 15240-062). The arrays were then left to rotate at 12 revolutions per h with a 15° inclination angle to allow air/CO_2 and medium to alternatively cover the slice. The medium was changed every 2–3 days. Using this technique, we have been able to maintain cultures for over a month with good morphology.

2.2. Hardware materials

In order to sample different subhippocampal fields, we used several multielectrode arrays, including the 8 × 8 multielectrode array design (MMEP-4, Gross et al., 1993), and the MEA system (Egert et al., 1998). The signals were amplified, recorded and analyzed using two different hardware and software setups. Multielectrode arrays permitted a spatio-temporal assessment of the neuronal activity in slices. They facilitated the search for the maximum output for a given input. The recorded responses were in the range of 10–100 μV/ms for the slope of evoked postsynaptic potentials (EPSPs) and 200–1500 μV for evoked population spike (PS) amplitude.

2.2.1. MEA hardware

The MEA system (www.multichannelsystems.com, Egert et al., 1998) consists of a 60-electrode array, pre-amps, and data acquisition hardware and software. The electrode conductors are gold based. The presented experiments were run using electrodes with a diameter of 30 μm and an inter-electrode distance of 200 μm. A special Ti–Au–TiN electrode interface provided low impedances in the range of 50 kΩ. Silicon nitride was used as the insulation layer. Data were sampled from every channel at 25 kHz and processed using MCS software (MCRack v 1.44). A separate stimulator box allowed a programmed stimulation of eight channels simultaneously.

2.2.2. MMEP hardware

The MMEP (Gross et al., 1993; Univ. North Texas, www.cnns.org) consists of a 64-electrode array, pre-amp, data acquisition board and a custom-designed software. The electrode conductors are formed from transparent but conductive Indium–Tin oxide on a soda-lime glass. The gold plated electrode tips (24×24 μm pads) are designed into an 8×8 formation (MMEP 4 design) with an inter-electrode distance of 150 μm. The insulation layer consists of polysiloxane resin layer. The average impedance is in the range of 0.8 MΩ at 1 kHz. Contacts at the periphery (32 from each side) were made possible using zebra strips. The signals were amplified $250\times$ using a custom made Plexon preamplifiers (www.plexoninc.com). Signals were later on channeled into two data Acquisition Boards (Microstar; DAP 3200/214e series) installed in parallel on a Pentium II 450M Hz personal computer. The need for another $10\times$ amplification reduced the sampling rate to a maximum of 136 μs (7.35 kHz) per channel. Since the total analog input a board could handle without multiplexing was 16, the total number of channels that could be studied was limited to 32 channels. The whole setup, except for the computer, was housed in a Faraday Cage on an antivibration table. The data acquisition boards were controlled by a custom written Matlab program (gui_microstar). Another graphic user interface for kernel analysis was written (gui_kernel). This program allowed simultaneous extraction and nonlinear analysis of the PSs for four different channels whose random input was the same.

2.2.3. Drug testing protocol

The intensity was set to produce 60–120% peak facilitation in the second order kernel. Once the intensity was set, five consecutive random trains were delivered to the Schaffer collaterals using an external Nichrome electrode. Each train consisted of 407 pulses, with two trains under control conditions and three under drug condition. The first two ensured the stationarity of the system, while the latter three assessed the time-dependent evolution of the drug effects.

3. Results

3.1. Characterization of spatio-temporal patterns of activity in acute and cultured hippocampal slices

In our experiments, we used acute as well as cultured hippocampal slices and two multi-electrode array systems, the MEA 60 from Multi-Channel Systems (Reutlingen, Germany) and the MMEP setup from Dr Gross. Both arrays consist of planar arrays of 60 electrodes etched on a glass surface through silicon micromanufacturing technology. The electrodes enable both stimulation and recording from slices. Similar arrays have been used by other groups for recording from acute (Novak and Wheeler, 1988; Oka et al., 1999) and cultured hippocampal slices (Stoppini et al., 1997; Egert et al., 1998), as well as cultured dissociated neurons (Gross et al., 1993; Jimbo et al., 1998). In general, it has been consistently reported that the characteristics of the electrophysiological responses obtained from MEAs are very similar to those obtained from conventional stimulation and recording techniques. The laminar structure of the hippocampus as well as the distribution of the electrodes in the MEA 60 (200 μm inter-pad spacing) are well suited to determine the flow of electrical activity in the so-called tri-synaptic hippocampal circuit, i.e. the sequential activation of the perforant path to dentate gyrus synapses, followed by the activation of the mossy fibers, and finally that of the Schaffer collateral pathway (Fig. 1). Depending on the location of the recording elements, field excitatory postsynaptic potentials (fEPSPs) or field PSs can be recorded. Note that these responses are identical to those obtained by traditional recording (Yeckel and Berger, 1998). In addition, several nonlinearities of the system exhibit similar properties whether they are studied on MEAs or with traditional approaches. Paired-pulse facilitation is easily demonstrated in field CA1 in response to stimulation in CA3, and its temporal properties are similar in acute slices and in slices cultured on the MEA or the MMEP systems (Fig. 2A and B). Similarly, paired-pulse facilitation was also observed in cultured slices (Fig. 2C), confirming earlier work that cultured slices manifest the same synaptic plasticity as in vivo preparations (Buchs et al., 1993; Muller et al., 1993).

Likewise, the ability to elicit long-term potentiation (LTP) in slices is a critical element to establish that the slices are 'healthy', and exhibit the complex cascades that are required to link network activity to modification of synaptic efficacy. An example of LTP in CA1 elicited in an acute slice by stimulation of the Schaffer collateral pathway at 100 Hz for 1 s is shown in Fig. 3A. LTP is also readily elicited in CA3 by electrical stimulation of the mossy fibers for 1 s at 10 Hz (Yeckel et al., 1999). We also routinely recorded LTP in CA3 following mossy fiber stimulation in cultured slices (Fig. 3C).

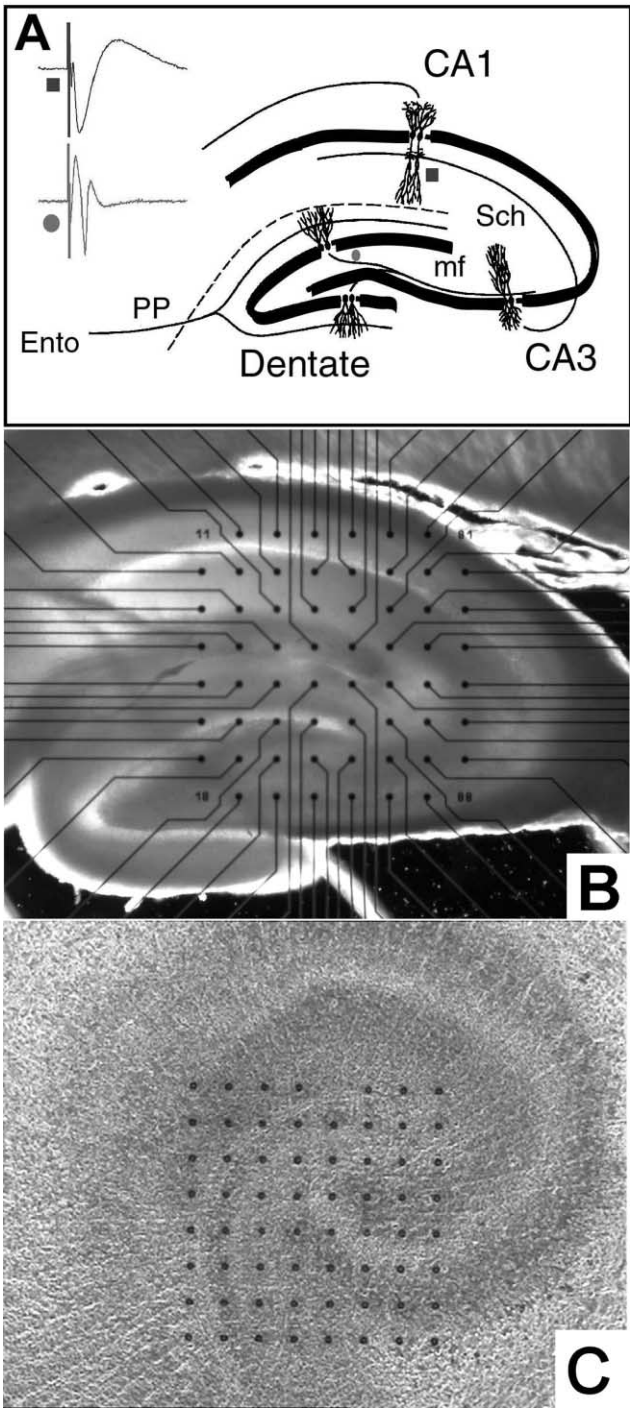

Fig. 1. (A) Schematic diagram of the tri-synaptic pathway in hippocampal slice. The Entorhinal cortex (Ento) provides the input to the Dentate Gyrus through the perforant pathway (PP) (synapse 1). The granule cells from the Dentate Gyrus send mossy fibers (mf) to the CA3 pyramidal cells (synapse 2), which extend their axons (Schaffer collaterals, Sch) to the CA1 pyramidal cells (synapse 3). The upper trace is a fEPSP that is evoked in the CA1 dentritic region in response to stimulation of the Schaffer collaterals. The lower trace shows a PS induced below the molecular layer of the dentate in response to perforant path stimulation. (B) Acute rat hippocampal slice positioned on the MEA array. (C) Two-week-old hippocampal slice cultured on the MMEP array.

As shown in Fig. 1B, the distribution of the recording pads on the MEA allows to sample the electrical activity over the entire tri-synaptic circuit of a rat hippocampal slice. Two-dimensional interpolated voltage frames were used to follow the flow of neuronal activation throughout the circuitry (Fig. 4). As can be seen in the figure, electrical stimulation of the mossy fibers produces a monosynaptic response in CA3, as well as a disynaptic one in CA1. The selected sequence of time frames in Fig. 4 shows the 2-D interpolated voltage distribution on the array as a result of the stimulation at the sites indicated in Fig. 4A. The frame number indicates the relative time in ms from the stimulus, which was considered to be at 0 ms. In this representation, the propagation of a negativity, which corresponds to the EPSP, can be traced from CA3 to CA1, and is followed by a spreading positivity, which corresponds to an hyperpolarization.

The conclusions of these studies are that hippocampal slices maintained in culture for weeks on the various multi-electrode arrays we have used are remarkably similar in their electrophysiological properties to acutely prepared hippocampal slices, and thus, the analytical tools developed with acutely prepared slices will be readily applicable to cultured slices.

3.2. Development of the random train stimulation for system characterization

Our goal is to quantify accurately the nonlinear characteristics of neuronal activity over time and online for two general purposes: (1) to identify biologically-based nonlinear dynamics for incorporation into biomimetic systems designed for pattern recognition and (2) to reliably detect systematic changes caused by exposure to chemical-biological agents. To achieve this goal, we have used a pseudorandom, broadband Poisson process stimulating pattern (Berger et al., 1988; Scalabassi et al., 1988; Iatrou et al., 1999) and advanced modeling techniques suitable for the rapid identification of the nonlinearities of the system from stimulus–response data. A basic premise of our approach is that functional characteristics of neuronal systems will be more pronounced in nonlinear descriptors (i.e. kernels of the functional power series), since the latter reflect the wide range of complex interactions among the multitude of biological mechanisms, both known and unknown, intrinsic to neuronal systems such as the hippocampus. It is these high-order nonlinearities that are most critical for identifying the extraordinary signal processing capabilities of the brain, and that will be highly sensitive for monitoring chemical–biological agent-induced alterations in higher cognitive processes.

In seeking a mathematical model for nonlinear stimulus–response relationships, we note that there is only

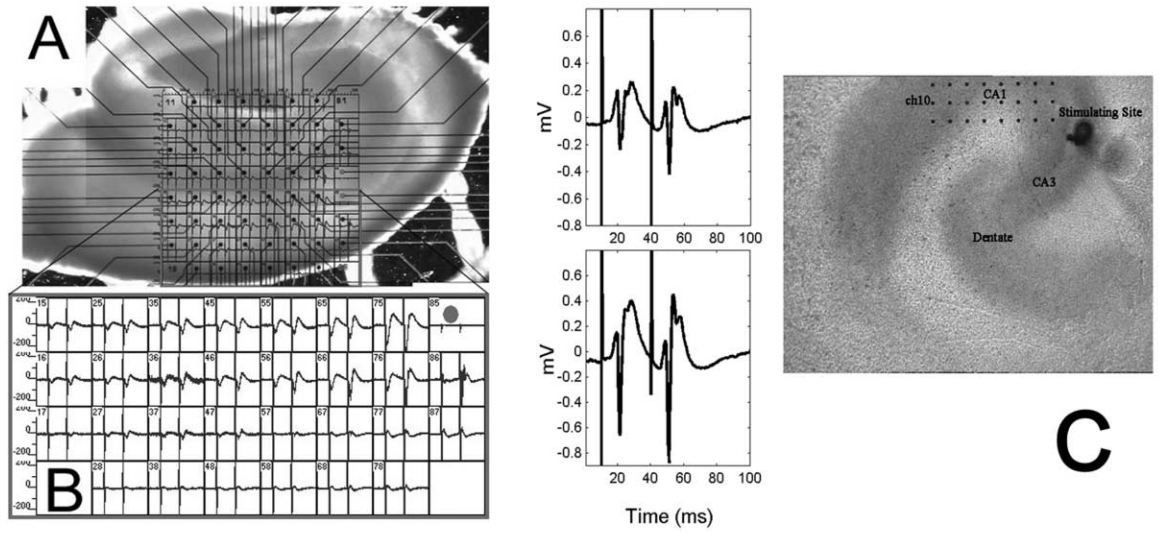

Fig. 2. Paired-pulse facilitation in acute slice (panels A and B) and cultured slice, respectively (panel C). (A) Paired pulse stimulation in the CA1 region, induced facilitation. The second EPSP is larger than the first one, and some second responses show a PS. (B) Enlarged figure showing the measured voltage at each electrode in a square. Paired pulses were delivered at 100 ms interval. Time scale is 150 ms per square, vertical scale is ± 250 μV per square. (C) Paired pulse facilitation of PSs in CA1 of a 2-week-old cultured slice. Paired pulse facilitation was observed in the CA1 of cultured slices, confirming earlier works that CA1 in vitro mature while retaining in vivo characteristics. Paired pulses were delivered at 30 ms interval. Horizontal time is in ms and the vertical scale is in mV.

one general model class with any realistic prospects for reliable estimation using real biological, i.e. noisy, data. This general class is the Volterra model that represents the response signal in terms of a hierarchical series of convolution integrals (summations for discrete-time data) containing kernel functions that characterize the nonlinearities of the system in ascending order of complexity (Volterra, 1930).

The Laguerre expansion of kernel (LEK) technique was introduced in the late seventies (Watanabe and Stark, 1975). It consists of a combination of least square estimation and a finite-dimensional approximation. The LEK technique, later refined in the early nineties (Marmarelis, 1993), presented several advantages over other methods. First, kernels up to the third order can be computed from a relatively short amount of data sets. Second, kernel estimates are robust to noise. Third, deviation of the input from strict whiteness does not alter the estimates. Fourth, the exponentially decaying orthonormal set of Laguerre functions allows the computed biological model to be electrically implemented using RC circuits.

In the LEK method, the output, $y(n)$, of a nonlinear discrete causal time invariant system can be given by the discrete Volterra series expansion represented by:

$$y(n) = c_0 + \sum_j c_1(j) \times v_j(n) + \sum_{j_1}\sum_{j_2} c_2(j_1, j_2) \times v_{j1}(n) \times v_{j2}(n) + \cdots, \quad (1)$$

$$v_j(n) = \sum_m b_j(m) \otimes x(n-m), \quad (2)$$

where x is the input and b_j form a set of orthonormal Laguerre base functions. The number of the coefficients (c_j) to be evaluated depends on the order of the system. The equation is equivalent to passing the input through a bank of linear filters b_j (Eq. (2)) and then applying a zero memory nonlinearity to get the output (Eq. (1)). These equations are best fit for a set of discretely sampled continuous input–continuous outputs.

Based on the Volterra modeling approach, we have now developed a time efficient method to estimate the nonlinearities in biological neuronal systems from impulse input–spike output datasets (Courellis et al., in preparation, Gholmieh et al., in preparation). The inputs and the outputs are sparse impulse sequences consisting of Poisson distributed electrical stimuli (inputs) and their corresponding PS amplitudes (outputs). In the new method, we remapped the problem by considering only the inter-stimulus intervals as inputs and the amplitudes of the PSs as the outputs, and we extended the Laguerre expansion method for estimating kernels (Marmarelis, 1993) according to:

$$y(n) = k_1\delta(n-n_i) + \sum_{n_i-\mu<n_j<n_i} k_2(n_i-n_j)\delta(n-n_i), \quad (3)$$

where δ denotes input impulses, n_i is the time of occurrence of the ith impulse, n_j is the time of occurrence of jth impulse before the ith impulse, $y(n)$ is the amplitude of the PS in response to an electrical pulse that occurred at time n_i, μ is the memory of the biological system, k_1 is the first order kernel, and k_2 is the second order kernel.

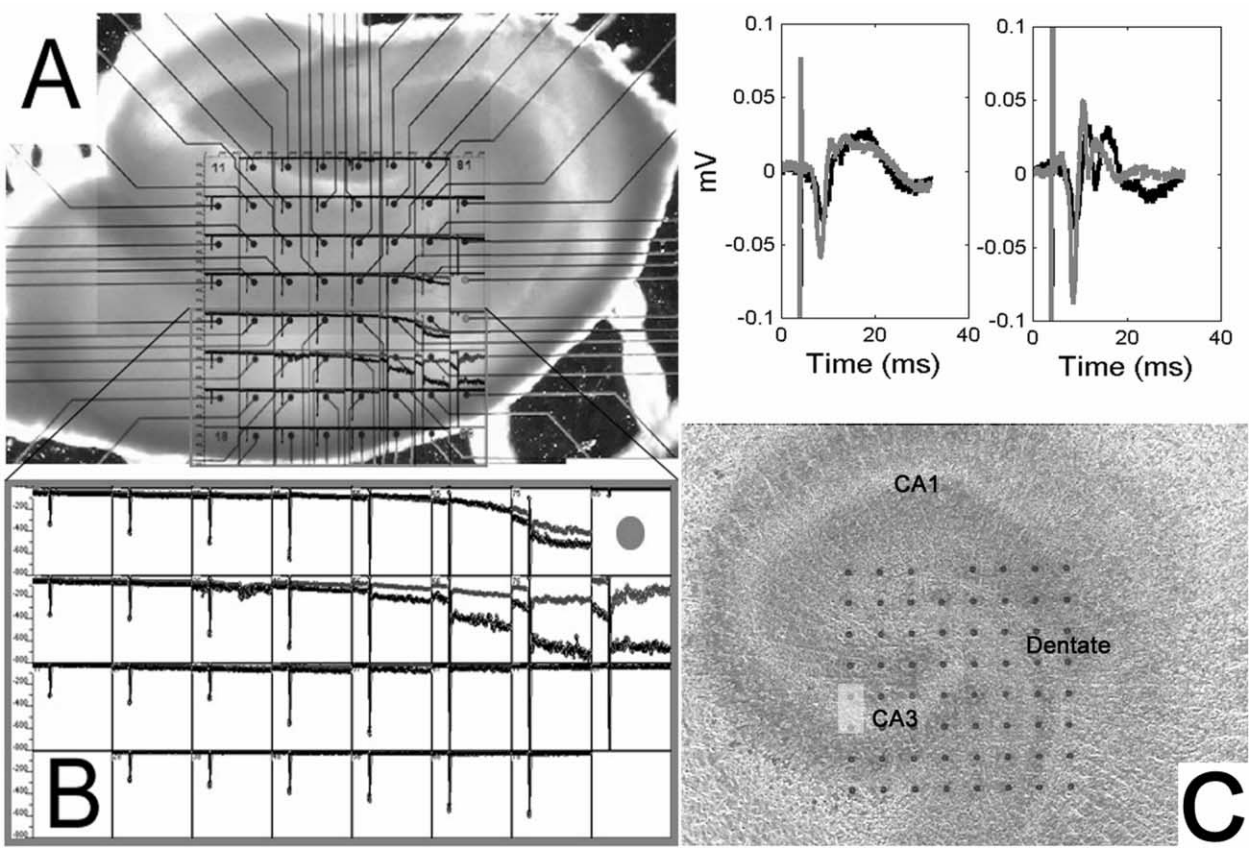

Fig. 3. LTP in acute (left panel) and cultured (right panel) hippocampal slices. (A and B) LTP is shown here in the CA1 region in a response to high-frequency stimulation (HFS). Test paired pulses (PP) were delivered every 50 s. The stimulation, at the black dots, consisted of two biphasic pulses of ± 75 μA for 100 μs each and with an interstimulus interval of 50 ms (see Fig. 2B). After 15 min of PP stimulation in a 100 μM picrotoxin containing aCSF, an HFS consisting of four trains of ten identical pulses at 100 Hz was delivered, following which PP stimulation was continued for over an hour. The graphs in panel B plot the minimum value of both the first (upper) and second (lower) EPSPs over the time course of the experiment. Each square shows the depth of the EPSP recorded for its corresponding electrode. Both first and second responses were potentiated after HFS (seen as increase in the EPSP depth after the vertical line artifact). The time scale is 1.15 h per square, while the vertical scale is ± 400 μV per square. (C) LTP was induced in CA3 of a cultured slice by a 1 s 10 Hz stimulation of the mossy fibers. LTP was assessed by overlaying averaged responses: pre (black) and post (after 1 h, gray) the 10 Hz stimulation. *Scale:* Time is in ms and amplitude is in mV.

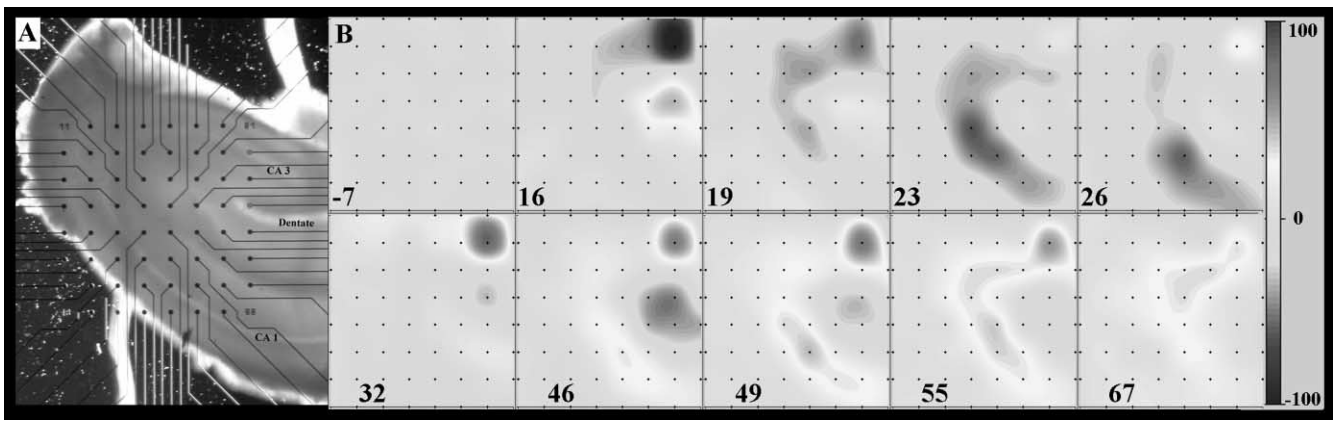

Fig. 4. Propagation of electrical activity in an acute hippocampal slice on the MEA system. The sequence of frames in (B) shows the 2-D interpolated voltage distribution on the array as a result of the stimulation of the slice shown in (A). Each frame captures 1/25 ms, and the stimulus was considered $t = 0$ ms. In this representation of the evoked response, the propagation of a negativity (deep gray, first row of frames) can be traced from CA3 to CA1, followed by a positivity (light gray, second row of frames). The negativity represents the postsynaptic potential spreading along the Schaffer collateral pathway, while the positivity represents the following hyperpolarization. Hilar stimulation (the two gray circles in the second frame) consisted of a biphasic pulse of ± 100 μA for 100 μs each. The gray scale bar on the right spanned 200 μV (100, -100 μV).

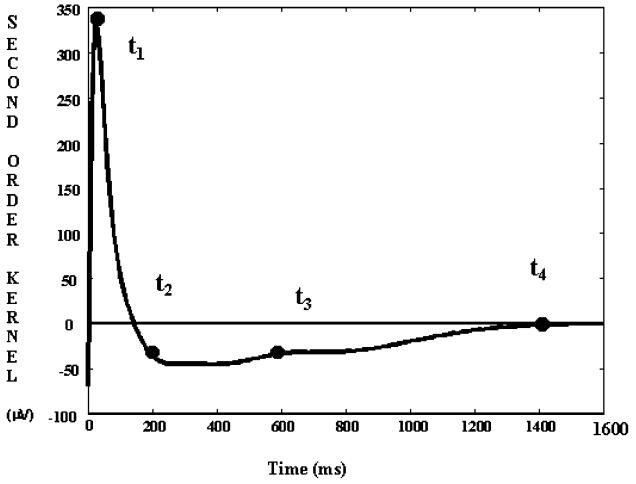

Fig. 5. Significance of the second order kernel. Second order kernels calculated for the PS amplitude elicited in CA1 by random train stimulation of the Schaffer collateral. The CA1 hippocampal system in vitro exhibits a fast rising facilitatory phase (0–30 ms), a peak between 20–50 ms, a fast facilitatory phase (30–200 ms) and a slow inhibitory relaxation phase (200–2000 ms). The memory of the second order kernel is in the range of 1600–2000 ms, that is, pulses that occurred 2000 ms before a certain pulse have no effect on the amplitude of the PS evoked by that pulse (Fig. 6). The small black circles are points of reference for Fig. 6.

The above equation describes the amplitude of the PS at time (n) in terms of the first order and second order kernels, the impulse evoking the PS, and the effect of past impulses. Using the Laguerre expansion method for L Laguerre basis functions, the second order kernel can be expressed as:

$$k_2(n_i - n_j) = \sum_{l}^{L} c_l L_l(n_i - n_j), \tag{4}$$

where L_l is the lth order Laguerre function and c_l is its corresponding coefficient.

Combining Eq. (3) and Eq. (4), we obtain:

$$\left\{ y(n_i) = k_1 + \sum_{l} c_l \sum_{j} L_l(n_i - n_j) \right\}_{i=1,\ldots,N}. \tag{5}$$

The coefficients c_l and the first order kernel (k_1) are estimated using the least square method. Substituting the estimated coefficients in Eq. (4), we obtain the estimate for the second order kernel (k_2). Figs. 5 and 6 illustrate the role of the first and second order kernels for calculating the amplitude of the PSs based on past impulses and the first and second order kernel estimates. The kernel estimates can be interpreted as follows: the first order kernel represents the mean of the PS amplitude, while the second order kernel represents the effect of the interactions between the current pulse and previous pulses on the amplitude of the PS. For example, if two impulses occurred at times n_i and n_j with $\boldsymbol{n_j > n_i}$, the second order kernel value at the interval ($\Delta t = n_i - n_j$) represents how the jth impulse

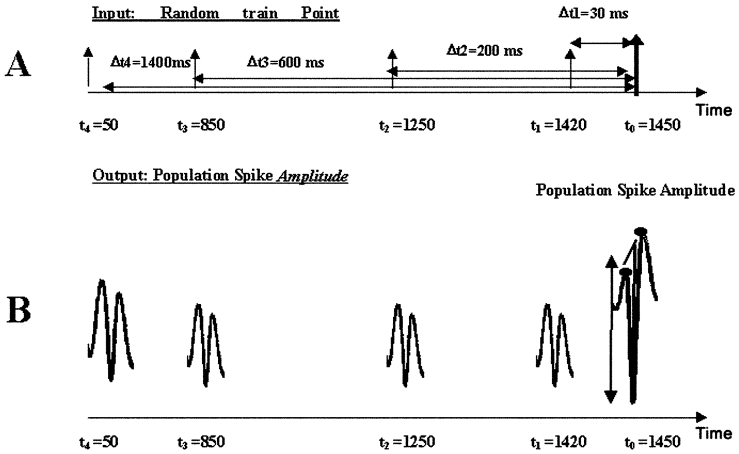

Fig. 6. Predictive power of first and second order kernels. (A) Series of input electrical stimuli applied through a stimulating electrode to the Schaffer collateral pathway. (B) The PS amplitudes corresponding to pulses of panel A. The amplitude of the response for the last stimulus (bold arrow, at 1450 ms) can be estimated using the first order kernel ($k_1 = 300$ μV), the second order kernel (Fig. 5), and Eq. (3)):

$$y(n) = k_1\delta(n - n_i) + \sum_{n_i - \mu < nj < n_i} k_2(n_i - n_j)\delta(n - n_i),$$

$$y(1450) = k_1 + k_2(1450 - 1420) + k_2(1450 - 1250) + k_2(1450 - 850) + k_2(1450 - 50),$$

$$= 300 + 340 - 30 - 30 + 0,$$

$$= 580\ \mu\text{V}.$$

Note: Time and amplitude are not drawn to scale. The amplitude of the PS is measured as the difference between the shortest distance between the minimum and the line that joins the two positive peaks. The response delays are not taken into consideration.

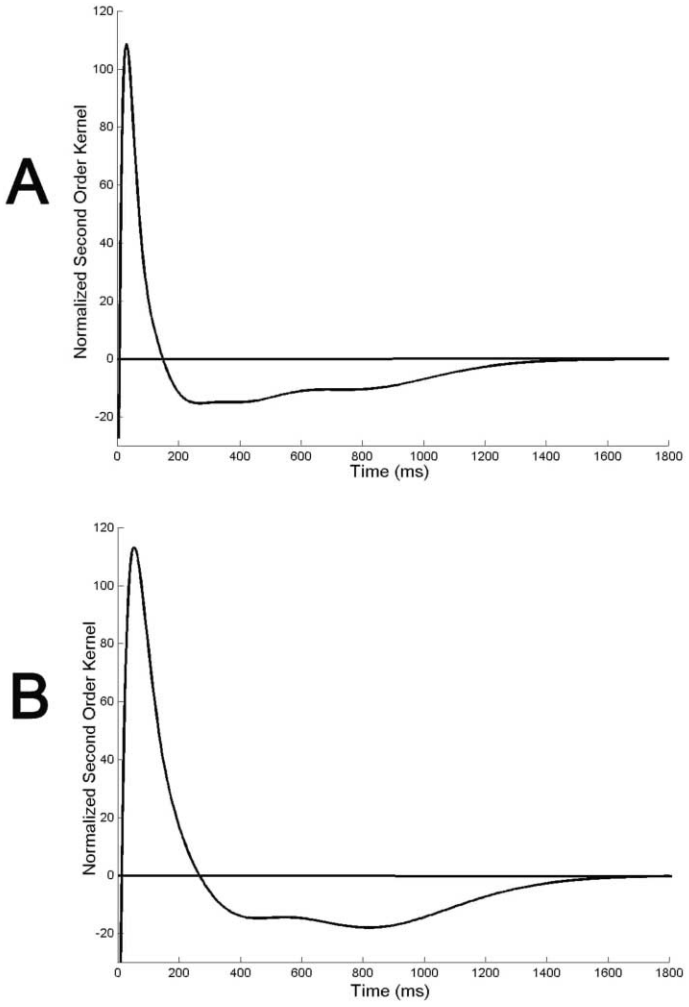

Fig. 7. Comparison of estimated second order kernels from acute (panel A) and cultured slices (panel B). The second order kernels from both preparations have the same characteristics as described in Fig. 5, i.e. they have an initial phase (0–50 ms), a peak of facilitation around 20–50 ms, and a late inhibitory phase (200–2000 ms).

modifies (i.e. increases or decreases) the PS amplitude response at time n_i. In contrast to paired pulse methods in which the interval between the two pulses is fixed, the second order kernel examines the effects of all possible intervals in an unbiased manner.

The second order kernel calculated for the PS amplitude elicited in CA1 by random train stimulation of the Schaffer collateral system exhibits a fast rising facilitatory phase (0–30 ms), a peak between 20–50 ms, a fast facilitatory phase (30–200 ms) and a slow inhibitory relaxation phase (200–2000 ms) (Figs. 5 and 6). The memory of the second order kernel is in the range of 1600–2000 ms, that is, pulses that occurred 2000 ms before a certain pulse have no effect on the amplitude of the PS evoked by that pulse. We also empirically determined that the characterization of the CA1 hippocampal system required nine Laguerre basis functions and impulse sequences of 3 min long, each with 407 pulses (Gholmieh et al., in preparation). Thus, every time a train of impulses is fed into the Schaffer collateral (CA1 input fibers), a set of ten variables are estimated: the first order kernel (k_1) and the value of the nine Laguerre coefficients. The normalized second order kernels (k_2/k_1) from acute and cultured slices were similar and showed the same degree of facilitation ($\cong 100\%$) (Fig. 7). On the other hand, the mean PS (k_1) was double in acute ($\cong 300$ μV) than in cultured slices ($\cong 150$ μV). The most probable reason for this difference is the smaller number of neurons in the cultured slice than in acute slices.

Several experiments were performed to establish the reliability of the technique to estimate the first and second order kernels as well as the nine coefficients of the Laguerre base functions (Fig. 8). Repeated trains of stimulation were delivered to the same slice or to different slices and the values of the coefficients averaged across repeats or across slices. In both cases, the data demonstrated a remarkable reproducibility of the estimates of the nine coefficients. These ten variables formed the basis for the quantitative evaluation and analysis of the effects of a drug on the system. As an illustration of this general approach, we determined the effects of the $GABA_A$ receptor antagonist, picrotoxin, on acute hippocampal slices (Fig. 9). As expected, 100 μM picrotoxin increased the value of the first order kernel by about 20%, and increased the degree of facilitation reflected by the positivity in the second order kernel within 10 min following picrotoxin addition to the perfusion medium. The feedforward inhibition of $GABA_A$ interneurons has, therefore, its maximum effect in the 20–50 ms range. When using the decomposition of the second order kernel into nine Laguerre base functions, picrotoxin produced a large and significant modification of several of the coefficients (up to 100%).

4. Discussion

Several of the requirements for a tissue-based biosensor have been implemented. First, we and others have established that the properties of electrophysiological responses from acute as well as cultured hippocampal slices are similar using several multi-electrode arrays and traditional electrophysiological techniques. In particular, the nonlinearities of the system, which form the basis for the sensitivity and discriminability of the biosensor, are similar in acute and cultured hippocampal slices. Second, we have established a new mathematical and computational tool to rapidly calculate the kernels of the Laguerre–Volterra expansion series. The new method generates a set of ten parameters to fully and reproducibly characterize the nonlinearities of the Schaffer collateral inputs to CA1 pyramidal neurons. Using this tool, we have demonstrated that picrotoxin

produces specific alterations in the second order kernels, thus illustrating the validity of our assumption that second order kernels represent a signature of the state of the system under various conditions. In preliminary experiments, we have also found that different drugs produced different alterations in second order kernels, further illustrating the power of the method. In particular, trimethylopropane (TMPP), a jet fuel residue that has been shown to act as a $GABA_A$ receptor antagonist (Kao et al., 1999), produced an effect that can be distinguished from that of picrotoxin. Third, we posit that the biosensor is sensitive, i.e. more sensitive than existing biosensors based on cultured neuronal cells, and discriminative, i.e. that the presence of different pharmacological agents results in different alterations of the state of the network that can be classified by the analytical tools we have developed. The advantage of the hippocampal slice culture over dissociated neuronal cultures is that the slice culture maintains the same neuronal circuit organization that is found in intact organisms, including humans. Thus, the culture preparation should be able to detect concentra-

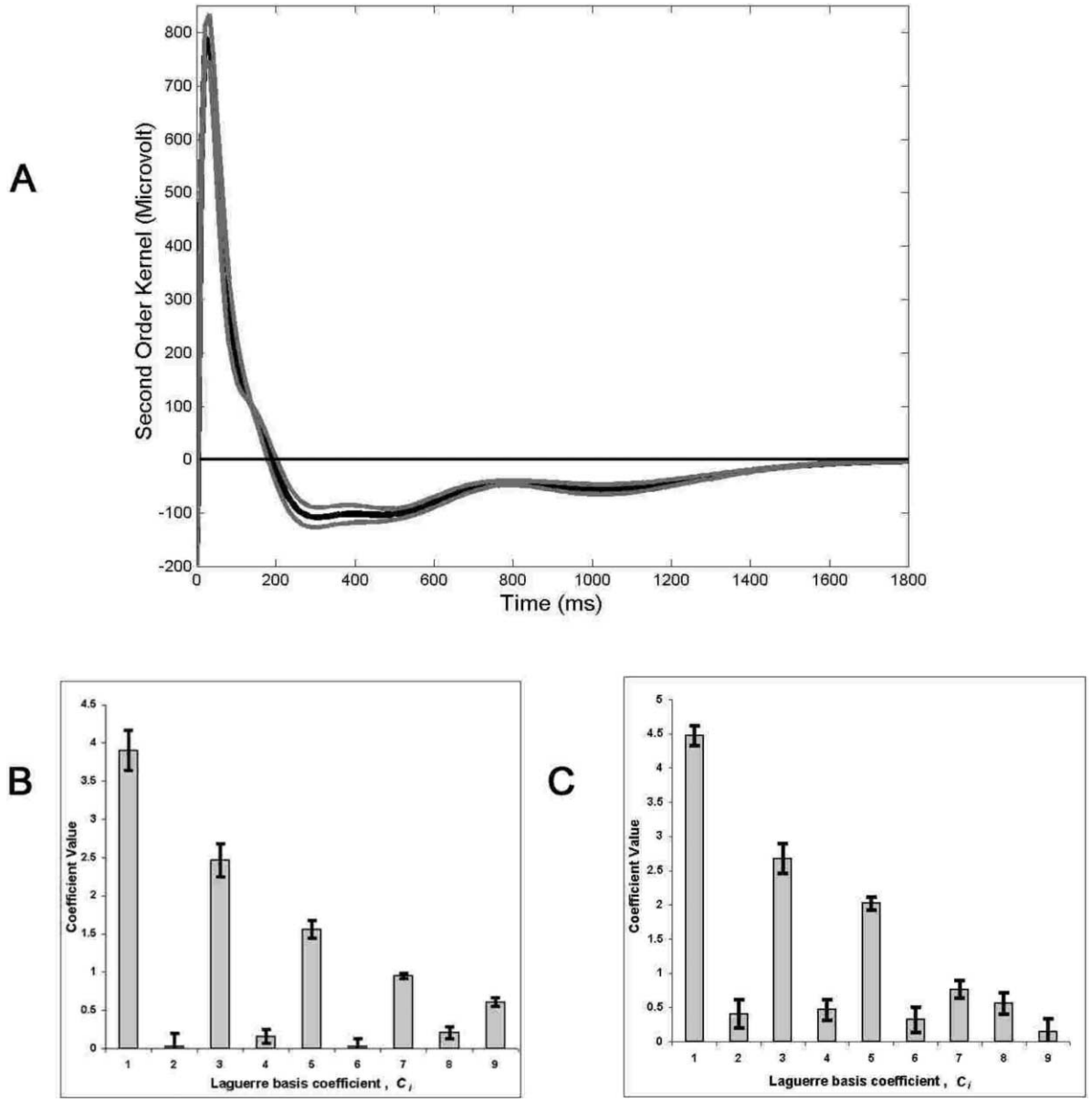

Fig. 8. Reproducibility of second order kernels within and between slices. According to the drug testing protocol, five successive random train stimulation (400 pulses each, delivered over 3 min) were delivered to the Schaffer collateral system and responses recorded in CA1 stratum radiatum. Second order kernels were determined as discussed in the text, and were averaged. (A) Average of five estimated second order kernels (black) delimited by 2 SD (gray). (B) Means (± 1 SD) of the corresponding nine Laguerre coefficients. (C) Means (± 1 SD) of the nine Laguerre coefficients obtained from six different slices and normalized with respect to peak facilitation. The estimated coefficients are unitless and are stable intra and across slices.

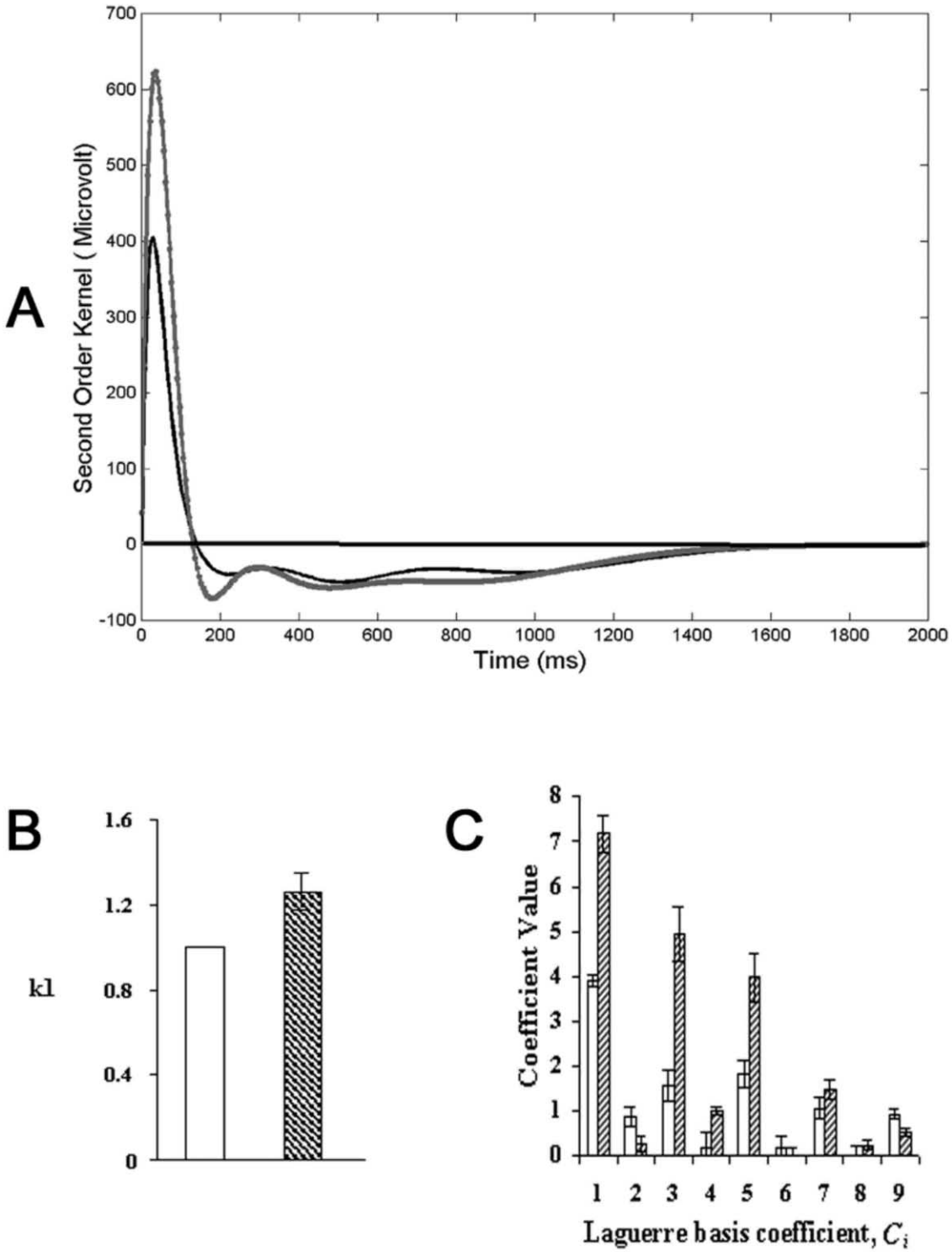

Fig. 9. Effects of picrotoxin (100 μM) on second order kernels. (A) Second order kernel before drug addition (black curve) and 15 min after perfusion with 100 μM picrotoxin (gray curve). (B) Effect of picrotoxin on first order kernel, k_1 (open bars: control; hatched bars: picrotoxin (100 μM); means ± SD of five experiments). (C) Effects of picrotoxin on the nine Laguerre basis coefficients (open bars: control; hatched bars: picrotoxin (100 μM); means ± SD of five experiments).

tions of drugs that are biologically significant, i.e. concentrations that are expected to affect biological functions carried on by the hippocampus. What remains to be established is to further expand on this approach and to show for instance that cross-kernel analysis obtained from random train stimulation using

two inputs—one output will provide for superior sensitivity and specificity. Finally, improved culture conditions are required for long-term recording and/or long-term storage of cultured slices leading to a real field-deployable biosensor.

Acknowledgements

This research was supported by grants from the Office of Naval Research (ONR), the Defense Advanced Research Projects Agency (DARPA), and the Biomedical Simulation Resource (BMSR).

References

Berger, T.W., Eriksson, J.L., Ciarolla, D.A., Scalabassi, R.J., 1988. Nonlinear systems analysis of the hippocampal perforant path-dentate projection. III. Comparison of random train and paired impulse stimulation. J. Neurophysiol. 60, 1095–1109.

Boppart, S.A., Wheeler, B.C., Wallace, C., 1992. A flexible perforated microelectrode array for extended neural recordings. IEEE Trans. Biomed. Eng. 39, 37–42.

Buchs, P.-A., Stoppini, L., Muller, D., 1993. Structural modifications associated with synaptic development in area CA1 of the rat hippocampal organotypic cultures. Dev. Brain Res. 71, 81–91.

Courellis, S.H., Marmarelis, V.Z., Berger, T.W. Modeling event-driven nonlinear dynamics in Biological Neural Systems, using impulse-sequence inputs and spike-train outputs. (in preparation).

Egert, U., Schlosshauer, H., Fennrich, S., Nisch, W., Fejtl, M., Knott, T., Muller, T., Hammerle, H., 1998. A novel organotypic long-term culture of the rat hippocampus on substrate–integrated multielectrode arrays. Brain Res. Protocol 2, 229–242.

Falkenrath, R.A., Newman, R.D., Thayer, B.A., 1998. America's Achiles' Heel: Nuclear, Biological, and Chemical Terrorism and Covert Attack. MIT Press, Cambridge.

Gahwiler, B.H., 1981. Organotypic monolayer cultures of nervous tissue. J. Neurosci. Meth. 4, 329–342.

Gross, G.W., 1979. Simultaneous single unit recording in vitro with a photoetched laser deinsulated gold multi-microelectrode surface. IEEE Trans. Biomed. Eng. 26, 273–279.

Gholmieh, G., Courellis, S.H., Marmarelis, V.Z., Berger, T.W. A novel method for modeling short-term synaptic plasticity. (in preparation).

Gross, G.W., Williams, A.N., Lucas, J.H., 1982. Recording of spontaneous activity with photoetched microelectrode surfaces from mouse spinal neurons in culture. J Neurosci. Meth. 5, 13–22.

Gross, G.W., Wen, F., Lin, W., 1985. Transparent indium tin oxide patterns for extracellular, multisite recording in neuronal culture. J. Neurosci. Meth. 15, 243–252.

Gross, G.W., Rhoadas, B.K., Reust, D.L., Schwalm, R.C., 1993. Stimulation of monolayer networks in culture through thin film indium-tin oxide recording electrodes. J. Neurosci. Meth. 50, 131–143.

Iatrou, M., Berger, T.W., Marmarelis, V.Z., 1999. Application of a novel modeling method to the nonstationary properties of potentiation in the rabbit hippocampus. Ann. Biomed. Eng. 27, 581–591.

Jimbo, Y., Robinson, H.P., Kawana, A., 1998. Strengthening of synchronized activity by tetanic stimulation in cortical cultures: application of planar electrode arrays. IEEE Trans. Biomed. Eng. 45, 1297–1304.

Kao, W.Y., Liu, Q.Y., Ma, W., Ritchie, G.D., Lin, J., Nordholm, A.F., Rossi, J., Barker, J.L., Stenger, D.A., Pancrazio, J.J., 1999. Inhibition of spontaneous GABAergic transmission by trimethylolpropane phosphate. Neurotoxicology 20, 843–849.

Maher, M.P., Pine, J., Wright, J., Tai, Y., 1999. The neurochip: a new multielectrode device for stimulating and recording from cultured neurons. J. Neurosci. Meth. 87, 45–56.

Marmarelis, V.Z., 1993. Identification of nonlinear biological systems using Laguerre expansions of kernels. Ann. Biomed. Eng. 21, 573–589.

Muller, D., Buchs, P.A., Stoppini, L., 1993. Time course of synaptic development in hippocampal organotypic cultures. Brain Res. Dev Brain Res. 71 (1), 93–100.

Meister, M., Pine, J., Baylor, D., 1994. Multi-neuronal signals from the retina: acquisition and analysis. J. Neurosci. Meth. 51, 95–106.

Novak, J.L., Wheeler, B.C., 1988. Multisite hippocampal slice recording and stimulation using a 32 element microelectrode array. J. Neurosci. Meth. 23, 149–159.

Oka, H., Shimono, K., Ogawa, R., Sugihara, H., Taketani, M., 1999. A new planar multielectrode array for extracellular recording: application to hippocampal acute slice. J. Neurosci. Meth. 93, 61–67.

Pine, J., 1980. Recording action potential from cultured neurons with extracellular microcircuit electrodes. J. Neurosci. Meth. 2, 19–31.

Rostker, B., 1997. Reported Detection of Chemical Agent. Camp Monterey, Kuwait.

Scalabassi, R.J., Eriksson, J.L., Port, R., Robinson, G., Berger, T.W., 1988. Nonlinear systems analysis of the hippocampal perforant path-dentate projection. I. Theoretical and interpretational considerations. J. Neurophysiol. 60, 1066–1076.

Stoppini, L., Duport, S., Correges, P., 1997. New extracelular multirecording system for the electrophysiological studies: application to hippocampal organotypic cultures. J. Neurosci. Meth. 72, 23–33.

Tucker, J.B., 2000. In: Tucker, J.B. (Ed.), Toxic Terror: Assessing Terrorist Use of Chemical and Biological Weapons (Basic Studies in International Security). MIT Press, Cambridge.

Volterra, V., 1930. Theory of the Functionals and of Integral and Integro-Differnetial Equations. Dover, New York.

Watanabe, B.A., Stark, L., 1975. Kernel method for non-linear analysis: investigation of a biological control system. Math. Biosci. 97, 99–108.

Yeckel, M.F., Berger, T.W., 1998. Spatial distribution of potentiated synapses in hippocampus: dependence on cellular mechanisms and network properties. J. Neurosci. 18 (1), 438–450.

Yeckel, M.F., Kapur, A., Johnston, D., 1999. Multiple forms of LTP in hippocampal CA3 neurons use a common postsynaptic mechanism. Nature Neurosci. 2, 625–633.